Research Article

Shuanglan Hu, Junsheng Huang, Dongting Huang, Peng Li, Jingjie Tang, and Fei Meng*

Increased flexibility to improve the catalytic performance of carbon-based solid acid catalysts

https://doi.org/10.1515/gps-2021-0059
received May 07, 2021; accepted September 01, 2021

Abstract: The correlation between catalytic performance and the structure of a carbon-based solid acid (G/F-1/x), an amorphous carbon-bearing SO_3H group, was investigated. Concentrated sulfuric acid was used to carbonize and sulfonate the mixed graphene and fructose powder for the preparation of carbon-based solid acid catalysts with different cross-linked structures. The results showed that the catalyst with a higher fructose loading amount presented higher catalytic performance. The catalytic performance improvement could be attributed to a high density of SO_3H groups and the fast diffusion of reactants and products enabled by a flexible carbon network. The best furfural yield was obtained up to 69.4% when the weight of graphene and the fructose loading ratio was 1:4.

Keywords: carbon-based solid catalysts, poor-cross-linking, furfural

1 Introduction

Solid acid catalysts have been widely used in the chemical industry because they are easy to recycle and reuse [1]. In addition, carbon-based solid acid catalysts have attracted the attention of researchers due to their easily accessible preparation resources as a wide range of biomass, stable products with excellent catalytic activity, and ease of structural modification as well as regulation [2–4]. Specifically, the amorphous carbon structure formed by incomplete carbonization of lignocellulose is used as an initial carbon matrix, and, following with acid modification, it becomes carbon-based solid acid catalysts with a graphite-like structure. These catalysts are widely used in hydrolysis, esterification, and dehydration condensation reactions [5–11].

Suganuma et al. found that this type of solid acid catalyst consisted of multiple graphite layers superimposed into sheets that were connected through methylene groups [12]. The smaller the size of the graphite sheet (carbon flakes formed by the incomplete carbonization of sugars), the more the active sites modified at the edge of sheets that are available for chemical reactions [13]. Lou et al. studied the effects of carbonization temperature and time length on the structure of carbon-based solid acid catalysts. Their study suggested that changing the preparation conditions of solid acid catalysts from biomass would significantly lead to alterations in catalysts' structure and subsequently affect their catalytic performance [14]. However, Nakajima and Hara reported that, within a certain temperature range, although an increase in the carbonization temperature would result in variable cross-links but has no effect on the size of the carbon flakes [15]. This meant that differences in catalytic performance due to changes in the carbonization temperature probably occurred because of the variations in cross-linking between the carbon flakes rather than changes in the size of the carbon flakes. Therefore, in order to reveal the deep-seated mechanism of the influence of the carbon layer structures on the catalytic efficiency of the carbon-based acid catalysts, we designed a series of catalysts with different patterns of cross-linking between the carbon layers and studied their catalytic efficiency as well.

Direct carbonization and sulfonation of sugar materials using concentrated sulfuric acid is a well-known simplified method for preparing carbon-based solid acid catalysts [16]. Given that the carbonization ability of concentrated sulfuric acid is not as good as calcination at high temperatures, the carbon frame body of the prepared carbon-based solid acid catalyst is usually fragile. Additionally, the structure is often unstable and the degree of graphitization is low. As speculated in the

* **Corresponding author: Fei Meng,** Guangdong Province Engineering Research Center for Green Technology of Sugar Industry, Institute of Bioengineering, Guangdong Academy of Science, No. 10 Shiliugang Road, Haizhu District, Guangzhou 510316, China, e-mail: gbimengfei@126.com
Shuanglan Hu, Junsheng Huang, Dongting Huang, Peng Li, Jingjie Tang: Guangdong Province Engineering Research Center for Green Technology of Sugar Industry, Institute of Bioengineering, Guangdong Academy of Science, No. 10 Shiliugang Road, Haizhu District, Guangzhou 510316, China

study, due to these shortcomings of sulfuric acid, the amorphous carbon structure obtained by carbonization using the concentrated form of the acid would rarely form graphite flakes with a complete crystalline structure. Instead, the structure would mainly consist of cross-linked aromatic carbons and short-chain alkanes.

Therefore, in this study, a series of solid acid catalysts with various degrees of graphitization were prepared by mixing different proportions of graphene and fructose before carbonization and sulfonation using concentrated sulfuric acid. The relationship between the catalytic activity and the structural softening of the carbon-based solid acid catalysts was then evaluated.

Furfural (FF) is generally produced from the hydrolysis of pentosane through the action of an acid to form pentose, which is then dehydrated and cyclized. The main raw materials for the production of FF include corncobs as well as other agricultural and sideline products. FF is the most important derivative of the furan ring system and could be synthesized through several methods. It is widely used in synthetic plastics, medicine, pesticides, and other industries. Additionally, many derivatives could be obtained from FF through oxidation, condensation, and other reactions on account of its active chemical properties. In this study, a reaction from xylose to FF was chosen as the model reaction [17].

2 Materials and methods

2.1 Materials

Graphene was purchased from Shenzhen Zhongsenlinghang Technology Co., Ltd., PR China (bulk density: 0.01–0.02 g·mL^{-1}, specific surface area: 50–200 m^2·g^{-1}, particle size: D90 11–15 μm, thickness: 1–3 layers, single layer rate: >80%). Fructose, H_2SO_4, xylose, FF, oleic acid, methyl oleate, and methyl heptadecanoate were purchased from Energy Chemical Co., Ltd., PR China. Methyl sulfoxide (DMSO), tetrahydrofuran (THF), methylene chloride (DMC), and methyl isobutyl ketone (MIBK) were purchased from Macklin Chemical Co., Ltd., PR China. All reagents used in this research were analytically pure and used without further purification.

2.2 Catalyst preparation

To prepare the solid acid catalysts, we mixed 1 g of graphene and a certain mass of fructose thoroughly and evenly, and then sulfonated the mixture with 10 mL of concentrated sulfuric acid (96% w/w) at 413 K under a N_2 atmosphere. The black powder obtained from sulfonation was washed and filtered repeatedly with hot deionized water to remove the residual sulfuric acid till the pH of the filtrate became neutral. Then, the filter residue was dried at 353 K for 12 h. These samples were denoted G/F-1/x, where x (x = 0.5 or 4) was the fructose loading mass.

2.3 Catalyst characterization

Conventional instrument characterization: scanning electron microscopy (SEM) images were recorded on a desktop scanning electron microscope (Phenom Pro-X, CN). FT-IR spectra were recorded on a Nicolet Nexus 670 with a resolution of 4 cm^{-1}. X-ray diffraction was analyzed on a Rigaku X-ray diffractometer system (XRD; Rint 2,000, Rigaku). The Raman spectra were recorded at a wavelength of 514 nm using the Renishaw inVia Laman microscope (UK) in which the objective was fixed at 4× with a 325 nm notch filter. The BET surface area and nitrogen adsorption–desorption isotherms were measured with a volumetric adsorption apparatus (ASAP 2460, USA). Solid-state NMR spectra were measured using a JNM-ECZ600R spectrometer (JP). The number of SO_3H groups bonded to the carbon materials was estimated by elemental microanalysis (LECO CS844, USA).

2.4 Acid–base titration analysis

The acid–base titration method was proposed for the determination of acidity and the acid radical volume of catalysts. Each titration experiment was repeated three times and the average value was taken as the experimental results. Phenolphthalein was used as an indicator in this acid–base titration. The amount of –OH groups is equal to the total acid amount – (the amount of $-SO_3H$ + –COOH), and the amount of –COOH group is equal to (SO_3H + –COOH) – ($-SO_3H$).

For the total acid titration ($-SO_3H$, –COOH, and –OH), 30 mg of the catalyst and 50 mL of 5 mmol·L^{-1} NaOH solution were added to a 100 mL Erlenmeyer flask and the reaction was stirred at room temperature for 24 h or ultrasonically shaken for 1 h. After filtering, 10 mL of the filtrate was pipetted and transferred to a 50 mL Erlenmeyer flask. The filtrate was then titrated with a 5 mmol L^{-1} HCl solution and the acid content of the catalyst was calculated referring to the volume consumed.

To determine the $-SO_3H$ content, 30 mg of the catalyst and 50 mL of a 2 mol·L^{-1} NaCl solution were added to a 100 mL Erlenmeyer flask, and the reaction was stirred at room temperature for 24 h or ultrasonically oscillated for 1 h. To determine the total content of $-SO_3H$ and $-COOH$, 30 mg of the catalyst and 50 mL of a 5 mol L^{-1} Na HCO_3 solution were added to a 100 mL conical flask, and the reaction was stirred at room temperature for 24 h or ultrasonically shaken for 1 h. After filtering, 10 mL of the filtrate was pipetted and transferred to a 50 mL Erlenmeyer flask. The filtrate was then titrated with 5 mmol L^{-1} NaOH solution, and the acid radical content of the catalyst was calculated referring to the volume consumed.

2.5 Swelling performance test

About 100 mg of the solid catalyst powder was put into 6 mm × 30 mm liquid-phase inserts of a flat-bottom glass tube and then centrifuged at 5,000 rpm for 10 min. The height of the powder (H_1) was measured, and then 200 µL of solvent (water) was added to the glass tube, stirred with a stainless steel wire, and kept vertically at room temperature for 24 h, The solution was then centrifuged again under the same conditions and then the height (H_2) of the powder after swelling was measured. The swelling degree $Q = H_2/H_1$.

2.6 Catalytic activity evaluation

The catalytic performance of the carbon-based solid acid catalyst samples was examined by performing the conversion of xylose to FF in water or in mixed liquor in a hydrothermal reactor with a Teflon inner tube. The solid loadings of the catalyst, xylose, and liquor were 150 mg, 750 mg, and 5 mL, respectively. The reaction solution was filtered with a syringe filter head (0.22 µm). The FF in the filtrate was analyzed by HPLC at 280 nm with an ultraviolet sensor and C18 chromatography column, and xylose was analyzed by HPLC with a Refractive Index and a Bio-red chromatography column. All data were averaged over three runs. The conversion and yield were calculated by the addition of the data measured in both organic and water phases.

Oleic acid (2.82 g, 0.01 mol), 0.64 g of methanol, and 50 mg of the solid catalyst were added to a 50 mL round bottom flask. The mixture was heated at 353 K in an oil bath (reflux condensation, magnetic stirring at 500 rpm). After the predetermined time (less than 8 h) of the reaction, samples of the reaction mixture (50 µL) were withdrawn from the upper phase and centrifuged, and then the supernatant liquid (5 µL) was mixed with 200 µL of methylheptadecanoate (internal standard) prior to GC analysis.

2.7 Reusability of the catalyst

The efficiency of the recycled catalyst was checked by reapplying it at least five times in the model reaction of xylose conversion at 423 K for 2 h. The catalyst was insoluble and easily separated by simple filtration and then washed with distilled water and ethanol to remove the adsorbed reactants and products. The recovered catalyst was dried each time by heating at 343 K for 12 h in a vacuum drying oven. Thus, the regenerated catalyst was reused till the end of the fifth reaction.

3 Results and discussion

3.1 Catalyst characterization

Figure 1 shows that with the increase in the amount of added fructose, the particle size became larger. In addition, the surface morphology of the prepared carbon catalysts showed that the particles were more stereoscopic rather than the representative graphite sheet structure. To perform SEM analysis, a metal sheet was used to roll flat each sample powder on the sample stage. As shown in Figure 1a–e, as the amount of fructose in the raw material increased, the prepared carbon catalyst became more rigid and difficult to be flattened using mechanical force. It is worth noting that the particle size discussed here is only the macroscopic size and not the microscopic carbon layer size. We first observed from the visible size that fructose could play the role of connecting graphite flakes. The more the fructose added to the raw material, the harder the carbon material's morphology. It was confirmed from the morphology picture that the smoother graphite sheet structure would be replaced by the massive carbon structure.

Figure 2a shows the FT-IR chromatogram of the prepared catalysts. From the infrared spectrum, all the prepared carbon-based solid acid catalysts contain sulfonic acid groups (1,042 and 1,167 cm^{-1}) and massive hydroxyl peaks (around 3,400 cm^{-1}). As shown in Figure 2b, according

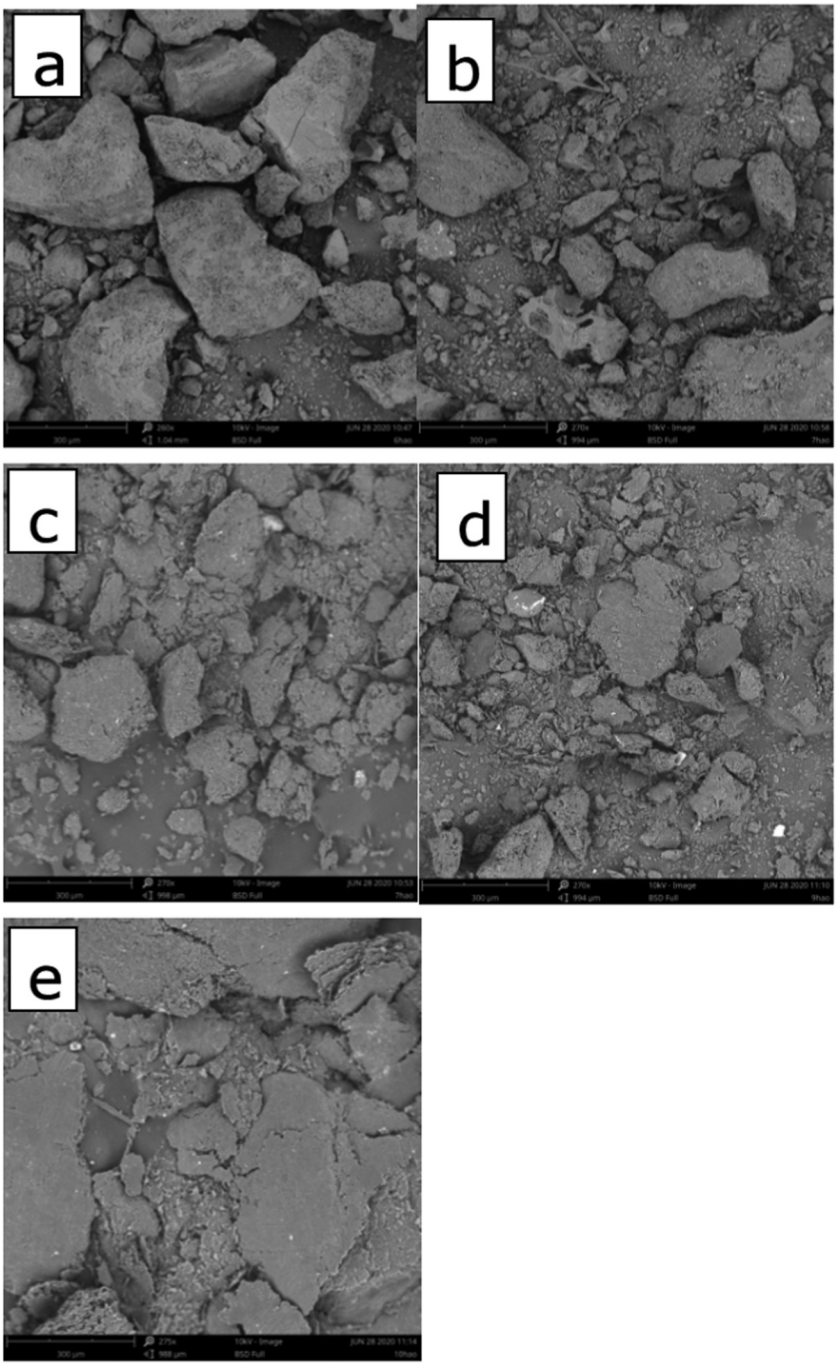

Figure 1: SEM images of the carbon solid acid catalysts prepared with different mass ratios of raw materials: (a) G/F-1/4, (b) G/F-1/3, (c) G/F-1/2, (d) G/F-1/1, and (e) G/F-1/0.5.

to the XRD pattern, the sharp peaks marked as 004 and 002 indicated the presence of crystalline graphite, and the peaks marked as 100 suggested the presence of an amorphous carbon structure. The wider the 100 peak width, the larger the size of the carbon sheet.

The Raman spectrogram was typically used in measuring the structure of carbon samples containing polycyclic aromatic carbon flakes (Figure 2c). As shown in Figure 2c, the peak around 1,570 cm^{-1} corresponds to the graphite peak (or G peak), a typical characteristic of the crystalline carbon. It was produced by the graphite base surface and acts as a strong tangential mode absorption band. Generally, the more developed the layer structure, the sharper the peak. Besides, the defect peak (or D peak) appearing at 1,350 cm^{-1}

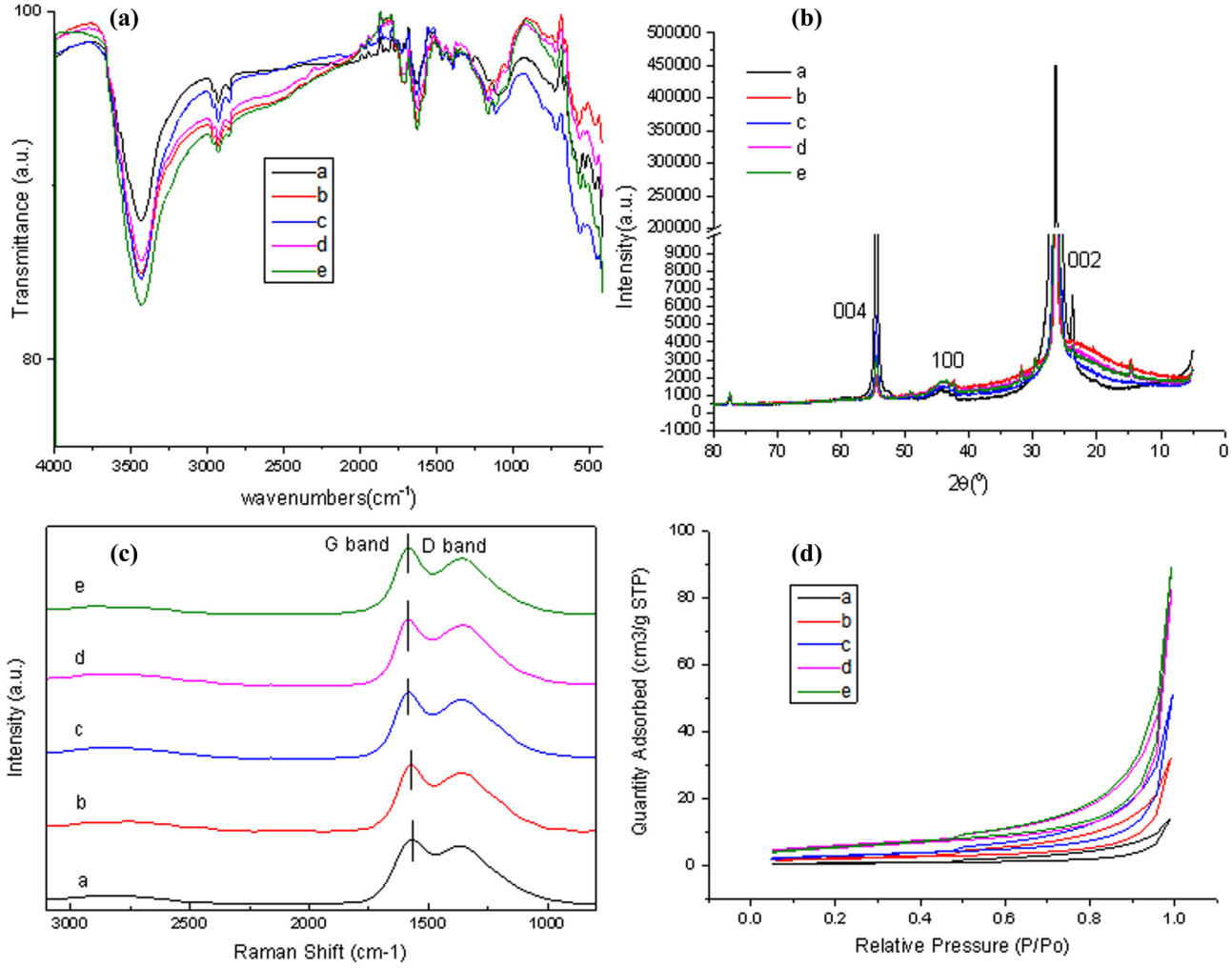

Figure 2: (a) FTIR spectra of the carbon solid acid catalysts prepared with different mass ratios of raw materials. (b) XRD results of the carbon solid acid catalysts prepared with different mass ratios of raw materials. (c) The Raman spectrum of the carbon solid acid catalysts prepared with different mass ratios of raw materials. (d) The BET curve of the carbon solid acid catalysts prepared with different mass ratios of raw materials: (a) G/F-1/4, (b) G/F-1/3, (c) G/F-1/2, (d) G/F-1/1, and (e) G/F-1/0.5.

Table 1: Structural parameters of carbon solid acid catalysts

Sample	C/H ratio[a]	SO_3H density ($mmol \cdot g^{-1}$)[a]	S_{BET} ($m^2 \cdot g^{-1}$)[b]	Pore size (nm)[b]	Nanoparticle size (nm)[b]	La (nm)[c]	G shift (cm^{-1})[c]	$R = I(D)/I(G)$[c]
G/F-1/4	31.17	0.53	3.4076	10.2979	1760.7795	12.8	1,567	0.902
G/F-1/3	32.54	0.59	7.7804	10.2310	771.1668	12.8	1,572	0.895
G/F-1/2	48.02	0.57	11.3636	9.2345	528.0014	12.8	1,582	0.894
G/F-1/1	56.35	0.61	19.4359	8.2229	308.7065	12.9	1,584	0.914
G/F-1/0.5	61.16	0.72	20.6967	8.7241	289.9008	12.9	1,582	0.911

[a]The C/H ratio and the amount of SO_3H groups are estimated by elemental analysis.
[b]The BET surface area and the nanoparticle size are estimated by BET analysis.
[c]La, G shift, and $R = I(D)/I(G)$ are estimated by Raman analysis.

was attributed to structural defects such as pentagons, heptagons, or other local defects. Then, the crystallization of the carbon material could be qualitatively characterized by referring to the intensity ratio of the G peak and D peak, namely $R = I(D)/I(G)$. Usually, the smaller the R-value we obtained according to Raman spectra, the more perfect the crystallization turned to be [18]. However, the $I(D)/I(G)$ value that stands for the degree of disorder in the carbon material presented no significant difference between each other according to our results (shown in Table 1, column 9).

Table 1 shows that the G position of these carbon solid acid catalysts shifted from 1,567 to 1,584 cm^{-1} when the mass ratio of graphene to fructose changed from 1:4 to 1:2. This was because although the formation of chemical bonds between the carbon elements was mainly sp^2 in graphene, the weak chemical bonds formed by fructose would decrease the vibration mode. The fructose addition would lead to a topological disorder (aliphatic and aromatic hydrocarbons) between the graphite sheets. Therefore, the position of the G peak in the catalysts with a large proportion of graphite moved toward a smaller value. It is noteworthy that although the structure difference of carbon materials could not be determined by the $I(D)/I(G)$ value, which only represents the degree of disorder, it could be estimated by the displacement of the G position since the connection form between carbon layers becomes softer due to the addition of the fructose raw materials.

According to the intensity ratio of the G and D bands, the average size of the carbon flakes in all the samples was estimated to be around 12.8 nm (La was approximately 12.8 nm, which stands for the size of the carbon sheets) [19]. The La value showing no obvious change indicated that the carbon sheets had not increased in size under different preparation conditions. However, as shown in Table 1, the C/H ratio also increased with the increasing proportion of graphene, which indicated that there was a change in the links between the carbon layers. This phenomenon might be caused by the accumulation of carbon layers with different proportions of graphene. A hypothesis suggests that concentrated sulfuric acid has a limited carbonization ability during the preparation process and does not affect the size of the carbon sheets in the prepared catalyst [20]. This phenomenon illustrated that under these experimental conditions, an increase in fructose did not cause a corresponding increase in the size of the carbon flakes but would result in variations in the type of cross-linking between the carbon flakes.

The content of sulfonic acid groups will affect the catalytic efficiency of the catalyst. Based on previous research studies, sulfonic acid groups tend to attach to the edge of the carbon layers. The increasing amounts of sulfonic acid groups in the sample G/F-1/0.5 might be attributed to the high C content (Table 1, column 3). Therefore, we speculated that the increasing amount of graphite has no significant effect on the sulfonic acid loading of the prepared catalyst. Additionally, there was no marked change observed in the size of the carbon layers (measured by the La value) between different catalysts, indicating that no additional carbon layer edges were formed for acid groups to attach. However, there was a distinct difference in the acid loading between these five prepared catalysts The results showed that the lower the fructose ratio, the higher the content of sulfonic acid groups. It was mainly because of two reasons. First, in the sulfonation reaction, fructose mainly would transform to amorphous carbon and the aromatic hydrocarbon carbon structure. Only a few graphite flakes transformed from fructose might be obtained among the ultimate carbon under this moderate carbonization level in our preparation process. As well known, the sulfonic acid groups in the catalysts mainly attach to the edge of the amorphous carbon layer [21] or are embedded between the graphene sheets [22]. The increase of fructose is not conducive to the increase of the attached sulfonic acid groups [23]. Therefore, the higher the proportion of graphene and the lower the proportion of fructose in the raw materials, the more sulfonic acid groups will be embedded. Second, when the fructose content in the raw material is high, the presence of hydroxyl and carboxyl groups in fructose decreases the carbon content when calculating the total amount of carbon in the prepared catalyst, When the proportion of carbon element decreases, the number of carbon atoms available to connect the sulfonic acid group also decreases from the overall perspective. Suppose we start the preparation at a fixed mass of carbon resource, namely the mixture of fructose and graphene, the ratio of carbon elements will decline with the increasing fructose proportion, and the catalyst as well as the proportion of sulfonic acid groups will all decline subsequently. That is to say, the proportions of sulfonic acid groups and carbon elements both decrease when the proportion of fructose in the raw material increases, and *vice versa*.

From the BET analysis (Figure 2d and column 4 in Table 1), we can see that as the content of graphene in the raw mixture increased, there was a gradual increase in the specific surface area of the prepared carbon material. The specific surface area of all the catalysts did not exceed the original specific surface area of the manufactured graphene purchased from Shenzhen. As shown in the results, without high temperatures, the carbonization

of fructose using concentrated sulfuric acid was not enough for the formation of a thin graphite sheet structure in the final catalyst. The role of fructose during the preparation was to soften the carbon structure of the final catalysts. This phenomenon is in line with our primary hypothesis when designing this experiment.

It can be seen from Figure 3a that a peak at 130 ppm, which represents the polycyclic aromatic carbons, has been observed in all catalysts. The characteristic peaks of phenolic OH (150 ppm) and COOH (172 ppm) were also vaguely visible. These two peaks might be caused by the oxidation of carbon by sulfonic acid [24–26]. The peaks at 30–110 ppm showed the presence of C–OH and C–O–C (72 ppm), CH_2, and CH– (102 ppm). These peaks might mainly be formed by fructose during carbonization, oxidation, and sulfonation, so they were more obvious in (c) G/F-1/2, (d) G/F-1/1, and (e) G/F-1/0.5 samples. From the size distribution results (Figure 3b), we can see that most of the catalyst particles are about 600–900 μm in size.

3.2 Catalytic activity

The increase in the specific surface area would generally favor chemical reactions in the water phase. By increasing the specific surface area, the distribution of reactants on the pores and surface of the catalyst becomes wider, which in turn improves the catalytic ability of the solid catalyst (per unit mass or unit volume) [27]. However, as the amount of graphene added to the raw materials increased, the catalytic performance of the prepared catalyst decreased (shown in Figure 4a). The highest yield of FF was obtained at 63.8% when the loading of graphene and fructose was 1 and 4 g, respectively. This suggested that these changes over several orders of magnitude in the specific surface area were not sufficient to alter the final yield of FF in these experiments. For example, BET results showed that the G/F-1/4 catalyst had the lowest specific surface area and the amount of sulfonic acid group among the five catalysts tested. But, the G/F-1/4 catalyst also obtained the best FF yield. As known, the specific surface area of the sugar-based carbon is significantly smaller than that of graphene, and there is a gap over several orders of magnitude. In contrast, the sugar-based catalyst is not inferior in terms of catalytic performance [5,6,28–30,32–37]. Thus, we speculate that the variations in the catalytic activity among these catalysts may be caused by changes in the methylene groups cross-linked between the carbon sheets.

The swelling of catalysts could facilitate the exposure of active groups and promote catalytic reactions. According to the swelling test, the more the fructose content in the raw material, the more pronounced the swelling effect of the prepared catalyst. As shown in Figure 5, the volume of the G/F-1/4 sample increased significantly after being immersed in water for 24 h. Unlike fructose, the catalyst from pure graphite does not contain polycyclic aromatic carbons. When pure graphite undergoes the same experimental process as the mixture of graphite and fructose, the volume of catalyst barely increases. The swelling property

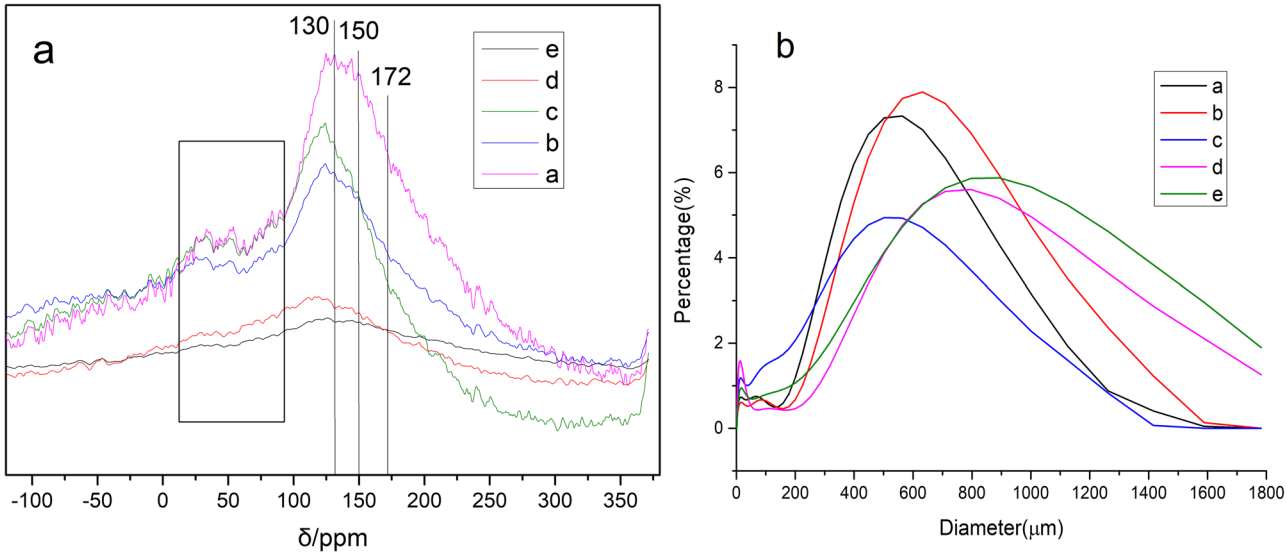

Figure 3: (a) The C^{13} NMR spectrum of the carbon solid acid catalysts prepared with different mass ratios of raw materials. (b) Size distribution results of the carbon solid acid catalysts prepared with different mass ratios of raw materials: (a) G/F-1/4, (b) G/F-1/3, (c) G/F-1/2, (d) G/F-1/1, (e) G/F-1/0.5.

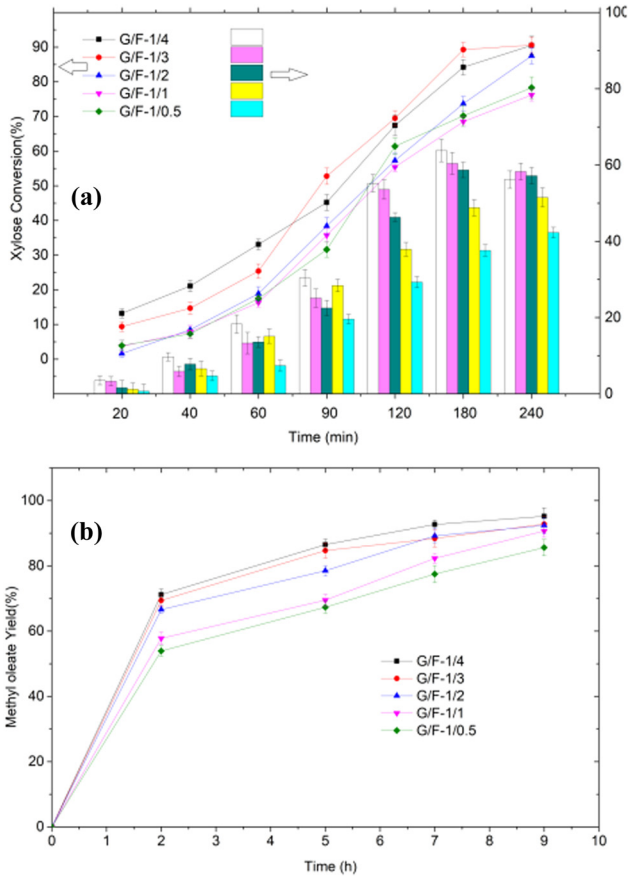

Figure 4: (a) Catalytic activities of the carbon solid acid catalysts prepared with different mass ratios of raw materials for the conversion from xylose to FF. (b) Catalytic activities of the carbon solid acid catalysts prepared with different mass ratios of raw materials for methyl esterification of oleic acid. Reaction conditions: (a) 423 K, 150 mg catalyst, 5 mL water, 750 mg xylose, (b) 353 K, 50 mg catalyst, 2.82 g oleic acid and 0.64 g methanol. Plots and lines represent the conversion rate of xylose; bars represent the FF yield.

difference between these catalysts indicated that the fructose in the raw materials could increase the ability of the reaction solvent to enter the catalyst carbon layer, and thereby further promote the contact between the reaction substrate and the catalytically active acid center.

We have calculated roughly the content of each group on the surface of the prepared carbon-based solid acid catalyst through a potentiometric titration test. Table 2 shows that the more fructose added to the raw material, the more carboxyl and hydroxyl groups would be present on the catalyst surface. It was reported that these hydrophilic groups are easily combined with hydroxyl-containing reaction substrates and can play a role in promoting the occurrence of reactions, thereby improving the catalytic efficiency of carbon-based catalysts. Comparing the data in Table 2 with Figure 4a, we found that the amount of the hydrophilic group content positively correlated with the catalytic efficiency of the catalyst. The affinity of the hydrophilic group to the substrate would promote the catalytic reaction. Besides, the carbon layer structure with hydrophilic groups becomes softer so that the reaction substrate is more likely to contact the

Table 2: Groups content of the prepared catalysts

Sample[a]	–OH (mmol·g^{-1})	–COOH (mmol·g^{-1})	–SO_3H (mmol·g^{-1})
G/F-1/4	0.24	0.13	0.57
G/F-1/3	0.23	0.15	0.63
G/F-1/2	0.22	0.11	0.62
G/F-1/1	0.18	0.09	0.66
G/F-1/0.5	0.14	0.06	0.74

[a]Groups are estimated by the acid–base titration.

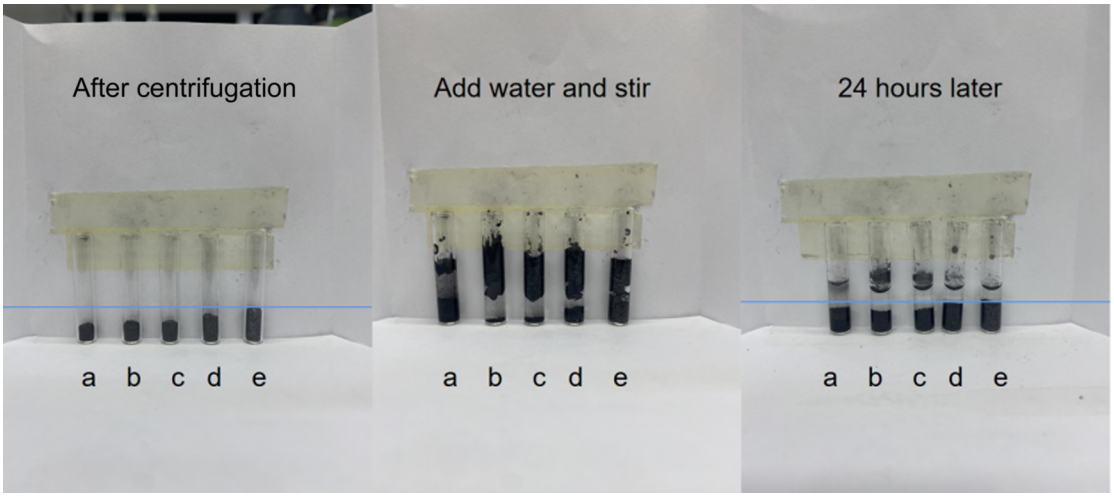

Figure 5: Swelling quantity of the carbon solid acid catalysts prepared with different mass ratios of raw materials. (a) G/F-1/4, (b) G/F-1/3, (c) G/F-1/2, (d) G/F-1/1, and (e) G/F-1/0.5.

active acid group. To further verify this hypothesis, we then applied the esterification reaction as a model reaction later.

Oleic acid is an unsaturated fatty acid with dominant hydrophobicity. It can react with methanol to produce methyl oleate. General acid catalysts can catalyze the esterification reaction. To further study the influence of the carbon sheet structure and hydrophilic groups of this type of carbon-based solid acid catalysts, we selected the esterification reaction of oleic acid and methanol as a model reaction for research. As shown in Figure 4b, before the reaction reaches equilibrium, the reaction rate always increased with the increase of the fructose content in the raw materials used for the preparation of the catalyst. The catalyzed esterification reaction obtained a yield of more than 85% when the reaction equilibrium conditions were reached. It is known that the main two factors affecting the reaction rate of the esterification reaction are as follows: the content of the acidic catalytic active center and the specific surface area of the catalyst. According to the researchers cited in ref. [28–30], when carbon-based solid acid catalysts are used in esterification reactions, the higher the acidity and the larger the specific surface area, the more efficient the reaction. As shown in Table 1, the porous pore diameters of these catalysts prepared were all greater than 8 nm, which almost reached the minimum pore size requirement for free access of oleic acid molecules. Therefore, there is no pore size restriction for the contact between the substrate and the catalytical active acid center.

The yield change trend of methyl oleate was consistent with that tendency of FF by those catalysts tested. Against common sense, although these two substrates had opposite hydrophilicity and hydrophobicity, the catalytic difference for these two reactions was not the opposite. This might be because the number of effective acid active centers has a greater influence on the catalytic performance than the characteristics of the product such as hydrophilicity and hydrophobicity.

It is well known that the position of the sulfonic acid group would also affect the catalytic performance of the catalyst. When forming a cationic graphene sheet–HSO_4–H_2SO_4 complex, even a large amount of sulfuric acid can be inserted between the large carbon (graphene) sheets in the well-crystallized graphite [22]. However, if the reaction substrate is not easily accessible to these intercalated sulfonic acid groups in the middle of the sheet, these sulfonic acid groups are still ineffective catalytically active groups for most reactions. It is well known that the properties of swelling agents would affect the diffusion of substrates in polymers, and this so-called "swelling" effect might also function in sulfonated carbon catalysts. Compared to smaller and more hydrophilic molecules such as FF and xylose, larger and more hydrophobic reactive species such as oleic acid are poor swelling agents, leading to a more extended induction period associated with the catalyst "swelling" requirements [31]. We, therefore, speculate that the content of ineffective acid groups has little influence on the catalytic efficiency of the prepared catalyst. Furthermore, the highly accessible sulfonic acid groups mainly exist in the soft carbon layer and the connection layer formed by the fructose raw material. Compared to the catalyst samples of the same mass unit, the sulfonic acid groups of G/F-1/4, which has softer carbon layers due to the addition of fructose raw materials according to the above characterization analysis results, would have more access positions. Of course, too much fructose added also has disadvantages, such as reduced stability and decreased specific surface area. In the future, we need to continue to conduct more in-depth research to determine the best ratio of raw materials during the preparation process.

3.3 Catalysts reusability

Reusability is an important property for the solid acid catalyst. In industry, the recycling of heterogeneous acid catalysts is of great significance to improve profitability and sustainability. To examine reusability, a five-run consecutive recycling experiment was conducted using xylose as a substrate. At the end of each run, catalysts were

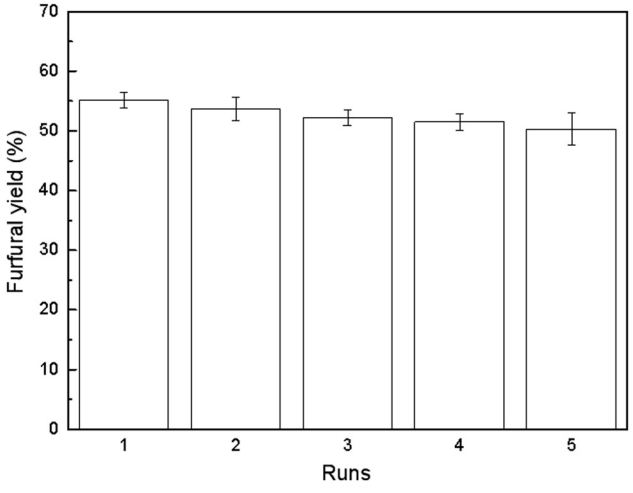

Figure 6: Reusability of the G/F-1/4 catalyst. Reaction conditions: 423 K, 150 mg G/F-1/4, 5 mL water, 750 mg xylose, 2 h.

Table 3: Element analysis of the recycled catalysts

Runs[a]	C/H ratio	C/% ($m \cdot m^{-1}$)	S/% ($m \cdot m^{-1}$)
Fresh	31.17	38.03	18.24
1	32.34	38.28	17.61
2	31.94	38.35	17.66
3	32.17	38.83	17.72
4	32.29	38.25	16.96
5	32.26	38.41	17.07

[a]C/H ratio, S, and C weight percent are calculated by elemental analysis.

filtered and washed with water and ethanol. Then, the recycled G/F-1/4 catalyst was dried at 343 K in a vacuum drying oven for several hours prior to reuse. Element analysis of the reused catalyst verified slight leaching of SO_3H after the 5th reuse. As shown in Figure 6, although some acid sites had been leached (Table 3), the FF yield remained stable with slight fluctuations in all recycling experiments, indicating the satisfactory hydrothermal stability and strong acid density of the G/F-1/4 catalyst during the conversion from xylose to FF.

3.4 Optimization of the reaction temperature and solvent

The effects of the reaction temperature and solvent on the yield of FF were studied. As well known, the temperature has a significant influence on the degradation of xylose. Therefore, we tested the performance of the G/F-1/4 catalyst at different reaction temperatures. It can be seen from Figure 7 that the too high reaction temperature (>443 K) would increase the reaction rate but at the same time cause a sharp drop in FF yield. Therefore, we choose 433 K as the reaction temperature condition for the following study.

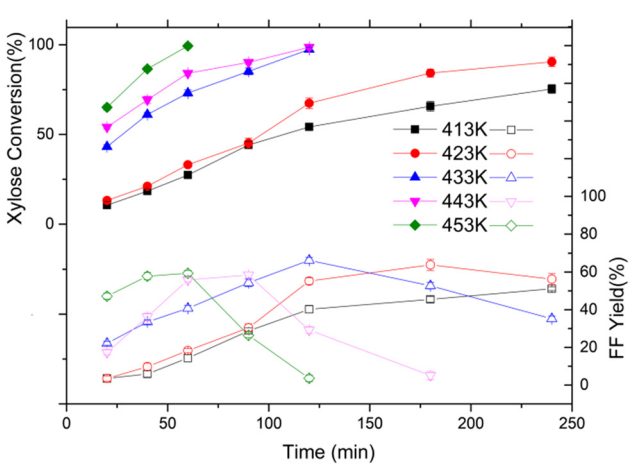

Figure 7: Effect of temperature on the conversion from xylose to FF. Reaction conditions: 150 mg G/F-1/4, 5 mL water, 750 mg xylose.

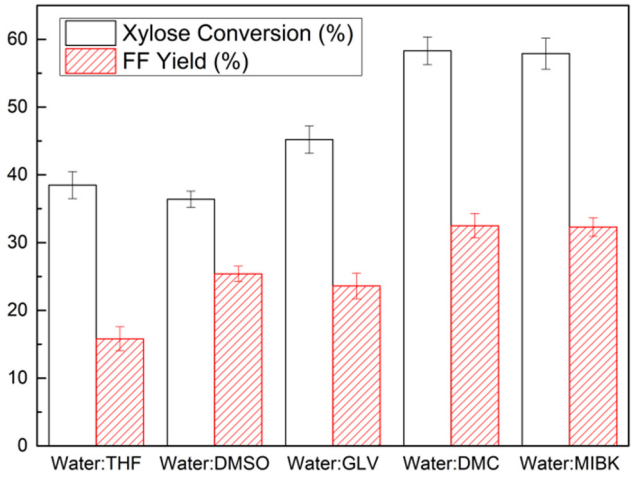

Figure 8: Effect of solvent on the conversion from xylose to FF. Reaction conditions: 433 K, 150 mg G/F-1/4, 5 mL solvent, 750 mg xylose.

Numerous studies have shown that a two-phase reaction system, formed by adding organic additives or organic solvents with water in the aqueous solution, can help increase the conversion rate of xylose and the yield of FF. Therefore, we tested the influence of several commonly used organic solvents on the catalytical reaction. As shown in Figure 8, in the two-phase systems, namely water/DMC and water/MIBK, the xylose conversion rate and the FF yield were significantly higher than those obtained from

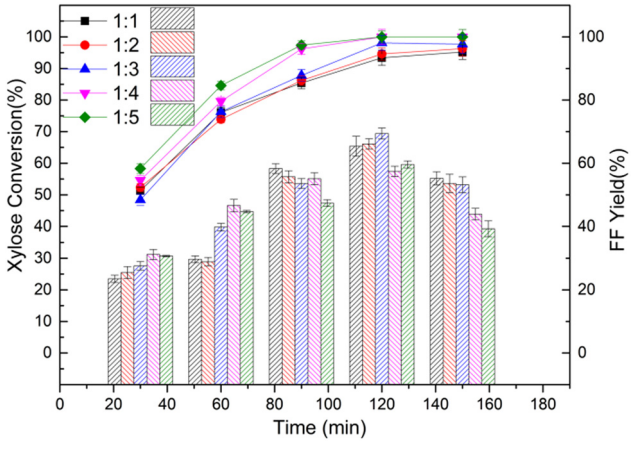

Figure 9: Effect of water content on the conversion from xylose to FF. Reaction conditions: 433 K, 150 mg G/F-1/4, 5 mL solvent, 750 mg xylose.

Table 4: Comparison of catalysts, reaction conditions, and FF yield

Catalyst	Reactions conditions	FF yield (%)	Ref.
Sulfonated GO	2.25 g xylose, 45 mg catalyst, 75 mg water, 473 K, 35 min	62	[32]
SCh	microwave-assisted, 1.0 mmol xylose, 15 mg SCh, 4 mL water-CPME (1:3, v/v), 463 K, 60 min	60	[33]
SO3H-NG-C	50 mg catalyst, 100 mg substrate, 5 mL GVL, 443 K, 20 min	74.4	[34]
SC-CaCt-700	45 mg SC-CaCt-700, 150 mg substrate, 7 mL GVL, 473 K, 100 min, 600 rpm	75 (xylose) 93 (corn stover)	[35]
Sg-CN	300 mg xylose, 50 mg catalyst, 2 mL water, 373 K, 30 min	96	[36]
SC-CCA	0.40 g xylose, 0.20 g catalyst, 16.5 mL GVL, 443 K, 30 min	79	[37]
FeClx-D008	0.1 g xylose, 4.9 g GVL, 0.01 g FeClx-D008, 4 MPa N_2, 403 K, 120 min	96.3	[38]
MC-SnOx-450 and NaCl	0.1 g MC-SnOx-450 in 1:1 (v/v) 20 g·L^{-1} xylose and 0.2 mol·L^{-1} NaCl aqueous phase/2-MTHF phase, 453 K, 20 min	53.9	[39]
pTSA-$CrCl_3$	1.0 M pTSA, 0.5 M $CrCl_3$, 50 mL DMSO, 393 K, 60 min	53.1	[40]
Al-SBA-15	0.9 g xylose, 0.1 g catalyst, 30 mL water, 15 bar N_2, 443 K, 5 h	60	[41]
G/F-1/4 catalyst	150 mg catalyst, 750 mg xylose, 5 mL water/DMC (1:3, v/v), 433 K, 2 h	69.4	This work

other solutions. Further, we studied the influence of the volume ratio of the water phase to the organic phase in the two-phase system on the catalytical reaction. As shown in Figure 9, the highest FF yield reached 69.4% when using a preferred carbon-based solid acid catalyst, using in a 1:3 water/DMC solution, and reacting at 433 K after 2 h.

3.5 Overall comparison with catalysts reported

The FF production of ten catalysts reported in other research studies is shown in Table 4. From Table 4, we can see that the optimal FF yield obtained by those catalysts prepared by sulfonating carbon was relatively low [32,33]. By doping the carbon source with elements [34–36] and changing the method of sulfonating reagents [37], the optimal FF yield becomes higher. The optimal FF yield and reaction time obtained by the catalyst in this work were not as excellent as those catalysts derived from resin [38], metal salts [39,40], and molecular sieves [41]. However, it was still higher than the type of sulfonated carbon-based catalyst.

4 Conclusion

This paper proposes a simple preparation method for increasing the flexibility of carbon-based solid acid catalysts and subsequently improving their catalytic efficiency for specific reactions. Furthermore, a batch of carbon-based solid acid catalysts with a flexible carbon layer cross-linked structure was prepared using fructose as raw materials. This study showed that flexibility in the connection between carbon layers had a significant effect on the catalytic efficiency of carbon-based solid acid catalysts during the conversion reaction from xylose to FF. We also used a variety of characterization techniques and experimental aids to verify the rationality of this design. Our results showed that the poor cross-linking facilitated the contact between the reaction substrate and the active catalytic center, and improved reaction rates.

Acknowledgements: The authors wish to acknowledge financial support from GDAS' Project of Science and Technology Development (2019GDASYL-0103042).

Funding information: The authors wish to acknowledge financial support from GDAS' Project of Science and Technology Development (2019GDASYL-0103042) and Special Project of Innovation Capacity Development of Guangdong Academy of Sciences (2018GDASCX-0105).

Author contributions: Shuanglan Hu: conceptualization, data curation, methodology, formal analysis, funding acquisition, writing – original draft; Junsheng Huang: investigation, project administration; Dongting Huang: formal analysis, software, visualization; Peng Li: validation, resources; Jingjie Tang: methodology, writing – original draft; Fei Meng: project administration, resources, funding acquisition, writing – review and editing.

Conflict of interest: The authors state no conflict of interest.

Informed consent: Informed consent has been obtained from all individuals included in this study.

Data availability statement: All data generated or analyzed during this study are included in this published article.

References

[1] Nagasuresh E, Srinivas D. Solid catalysts for conversion of furfural and its derivatives to alkanediols. Chem Rev. 2020;62(6):1–41. doi: 10.1080/01614940.2020.1744327.

[2] Qi W, He C, Wang Q, Liu S, Yu Q, Wang W, et al. Carbon-based solid acid pretreatment in corncob saccharification: specific xylose production and efficient enzymatic hydrolysis. ACS Sustain Chem Eng. 2018;6(3):3640–8. doi: 10.1021/acssuschemeng.7b03959.

[3] Cao Y, Liang D, Zhang H. Biomass-derived N-doped porous two-dimensional carbon nanosheets supported ruthenium as effective catalysts for the selective hydrogenation of quinolines under mild conditions. Catal Commun. 2020;143(5):106048. doi: 10.1016/j.catcom.2020.106048.

[4] Chen Y, Ai X, Huang B, Huang M, Huang Y, Lu Y. Consecutive preparation of hydrochar catalyst functionalized in situ with sulfonic groups for efficient cellulose hydrolysis. Cellulose. 2017;24:2743–52. doi: 10.1007/s10570-017-1306-x.

[5] Marina G, Rodrigo B, Inês M, Maria B, Isabel MF, Elena P. Porous carbons-derived from vegetal biomass in the synthesis of quinoxalines. Mechanistic insights. Catal Today. 2019;354:90–9. doi: 10.1016/j.cattod.2019.06.043.

[6] Gong R, Ma Z, Wang X, Han Y, Gou Y, Sun G, et al. Sulfonic-acid-functionalized carbon fiber from waste newspaper as a recyclable carbon based solid acid catalyst for the hydrolysis of cellulose. RSC Adv. 2019;9:28902–7. doi: 10.1039/C9RA04568F.

[7] Min S, Duan Y, Li Y, Li Y, Wang F. Biomass-derived self-supported porous carbon membrane embedded with Co nanoparticles as an advanced electrocatalyst for efficient and robust hydrogen evolution reaction. Renew Energy. 2020;155:447–9. doi: 10.1016/j.renene.2020.03.164.

[8] Sangar SK, Lan CS, Razali SM, Farabi MSA, Yun HT. Methyl ester production from palm fatty acid distillate (PFAD) using sulfonated cow dung-derived carbon-based solid acid catalyst. Energy Convers Manag. 2019;196(15):1306–15. doi: 10.1016/j.enconman.2019.06.073.

[9] Zhang Q, Xiang X, Ge Y, Yang C, Zhang B, Deng K. Selectivity enhancement in the g-C_3N_4-catalyzed conversion of glucose to gluconic acid and glucaric acid by modification of cobalt thioporphyrazine. J Catal. 2020;388:11–9. doi: 10.1016/j.jcat.2020.04.027.

[10] Zhu Y, Huang J, Sun S, Wu A, Li H. Effect of dilute acid and alkali pretreatments on the catalytic performance of bamboo-derived carbonaceous magnetic solid acid. Catal. 2019;9(3):245. doi: 10.3390/catal9030245.

[11] Sun K, Zhou Y, Xu X, Li Y, Hu Y, Li L.et al. Lignin-derived graphene-like carbon nanosheets as an efficient catalyst support for Fischer-Tropsch synthesis. J Nanosci Nanotech. 2020;20(10):6512–6. doi: 10.1166/jnn.2020.17893.

[12] Suganuma S, Nakajima K, Kitano M, Hayashi S, Hara M. sp(3)-linked amorphous carbon with sulfonic acid groups as a heterogeneous acid catalyst. Chem Sus Chem. 2012;5:1841–6. doi: 10.1002/cssc.201200010.

[13] Fukuhara K, Nakajima K, Kitano M, Kato H, Hayashi S, Hara M. Structure and catalysis of cellulose-derived amorphous carbon bearing SO_3H groups. Chem Sus Chem. 2011;4:778–84. doi: 10.1002/cssc.201000431.

[14] Lou W, Guo Q, Chen W, Zong M, Wu H, Thomas JS. A highly active Bagasse-derived solid acid catalyst with properties suitable for production of biodiesel. Chem Sus Chem. 2012;5:1533–41. doi: 10.1002/cssc.201100811.

[15] Nakajima K, Hara M. Amorphous carbon with SO_3H groups as a solid Brønsted acid catalyst. ACS Catal. 2012;2:1296–9. doi: 10.1021/cs300103k.

[16] Li M, Chen D, Zhu X. Preparation of solid acid catalyst from rice husk char and its catalytic performance in esterification. Chin J Catal 2013;34:1674–9. doi: 10.1016/S1872-2067(12)60634-2.

[17] Delbecq F, Wang Y, Muralidhara A, Quardi KE, Marlair G, Len C. Hydrolysis of hemicellulose and derivatives-a review of recent advances in the production of furfural. Front Chem. 2018;6:146. doi: 10.3389/fchem.2018.00146.

[18] Ferrari AC, Robertson J. Raman spectroscopy of amorphous, nanostructured, diamond-like carbon, and nanodiamond. Philos Trans R Soc a-Mathematical Phys Eng Sci. 2004;362:2477–512. doi: 10.1098/rsta.2004.1452.

[19] Ferrari AC, Robertson J. Interpretation of Raman spectra of disordered and amorphous carbon. Hysical Rev B. 2000;61(20):14095–107. doi: 10.1103/PhysRevB.61.14095.

[20] Kumar A, Patil S, Joshi A, Bhoraskar V. Mixed phase, sp(2)-sp(3) bonded, and disordered few layer graphene-like nanocarbon: synthesis and characterizations. Appl Surf Sci. 2013;271:86–7. doi: 10.1016/j.apsusc.2013.01.097.

[21] Lakhya JK, Päivi M, Eero S, Narendra K, Ashim JT, Mikkola J, et al. Towards carbon efficient biorefining: multifunctional mesoporous solid acids obtained from biodiesel production wastes for biomass conversion. Appl Catal B-Environ. 2015;176:20–35. doi: 10.1016/j.apcatb.2015.03.005.

[22] Mai O, Atsushi T, Masakazu T, Junko NK, Kazunari D, Takashi T, et al. Acid-catalyzed reactions on flexible polycyclic aromatic carbon in amorphous carbon. Chem Mater. 2006;18:3039–45. doi: 10.1021/cm0605623.

[23] Fredrik B, Niklas H. Microporous humins prepared from sugars and bio-based polymers in concentrated sulfuric acid. ACS Sustain Chem Eng. 2019; 7:1018–27. doi: 10.1021/acssuschemeng.8b04658.

[24] Nakajima K, Hara M. Environmentally Benign Production of Chemicals and Energy Using a carbon-based strong solid acid. J Am Ceram Soc. 2007;90(12):3725–34. doi: 10.1111/j.1551-2916.2007.02082.x.

[25] Cai W, Richard DP, Frank J, Sungjin P, Medhat AS, Yoshitaka I, et al. Synthesis and solid-state NMR structural characterization of 13C-labeled graphite oxide. Science. 2008;321:1815–7. doi: 10.1126/science.1162369.

[26] Sungjin P, Hu Y, Jin OH, Lee H, Leah BC, Cai W, et al. Chemical structures of hydrazine-treated graphene oxide and generation of aromatic nitrogen doping. Nat Commun. 2012;3:1–8. doi: 10.1038/ncomms1643.

[27] Gao Y, Liu Z, Gao R, Hu G, Zhao J. Support ionic liquid-heteropolyacid hybrid on mesoporous carbon aerogel with a high

surface area for highly efficient desulfurization under mild conditions. Micropor Mesopor Mat. 2020;305:11039221. doi: 10.1016/j.micromeso.2020.110392.
[28] Lou W, Zong M, Duan Z, Efficient production of biodiesel from high free fatty acid-containing waste oils using various carbohydrate-derived solid acid catalysts. Bioresour Technol. 2008;99(18):8752–7. doi: 10.1016/j.biortech.2008.04.038.
[29] Azeem R, Mohammed SMA, Mohammed MA, Rashed SB, Chanbasha B, Abdulaziz AA. Preparation and characterization of biomass carbon–based solid acid catalysts for the esterification of marine algae for biodiesel production. Bioenerg Res. 2019;12:433–42. doi: 10.1007/s12155-019-9965-0.
[30] Song X, Fu X, Zhang C, Huang W, Zhu Y, Yang J, et al. Preparation of a novel carbon based solid acid catalyst for biodiesel production via a sustainable route. Catal Lett. 2012;142:869–74. doi: 10.1007/s10562-012-0840-2.
[31] Wu J, Hua W, Yue Y, Gao Z. Swelling characteristics of g-C_3N_4 as base catalyst in liquid-phase reaction. Acta Phys Chim Sin. 2020;36(1):1904066–7. doi: 10.3866/PKU.WHXB201904066.
[32] Lam E, Chong JH, Majid E, Liu Y, Hrapovic S, Leung ACW, et al. Carbocatalytic dehydration of xylose to furfural in water. Carbon. 2012;50:1033–43. doi: 10.1016/j.carbon.2011.10.007.
[33] Wang Y, Delbecq F, Kwapinski W, Len C. Application of sulfonated carbon-based catalyst for the furfural production from D-xylose and xylan in a microwave assisted biphasic reaction. Mol Catal. 2017;438:167–72. doi: 10.1016/j.mcat.2017.05.031.
[34] Yang T, Li W, Ogunbiyi AT, An S. Efficient catalytic conversion of corn stover to furfural and 5-hydromethylfurfural using glucosamine hydrochloride derived carbon solid acid in Y-valerolactone. Ind Crop Prod. 2021;161:113173–9. doi: 10.1016/j.indcrop.2020.113173.
[35] Li W, Zhu Y, Lu Y, Liu Q, Guan S, Chang HM, et al. Enhanced furfural production from raw corn stover employing a novel heterogeneous acid catalyst. Bioresour Technol. 2017;245:258–65. doi: 10.1016/j.biortech.2017.08.077.
[36] Verma S, Baig N, Nadagouda MN, Len C, Varma RS. Sustainable pathway to furanics from biomass via heterogeneous organo catalysis. Green Chem. 2017;19:164–5. doi: 10.1039/c6gc02551j.
[37] Zhang T, Li W, Xu Z, Liu Q, Ma Q, Jameel H, et al. Catalytic conversion of xylose and corn stalk into furfural over carbon solid acid catalyst in γ-valerolactone. Bioresour Technol. 2016:209:108–14. doi: 10.1016/j.biortech.2016.02.108.
[38] Sun K, Shao Y, Liu P, Zhang L, Gao G, Dong D, et al. A solid iron salt catalyst for selective conversion of biomass-derived C-5 sugars to furfural. Fuel. 2021;300:120990. doi: 10.1016/j.fuel.2021.120990.
[39] Zhou N, Zhang C, Cao Y, Zhan J, Fan J, Clark J, et al. Conversion of xylose into furfural over MC-SnOx and NaCl catalysts in a biphasic system. J Clean Prod. 2021;331:127780. doi: 10.1016/j.jclepro.2021.127780.
[40] Sajid M, Dilshad MR, Rehman MSU, Liu DH, Zhao XB. Catalytic conversion of xylose to furfural by p-Toluenesulfonic Acid (pTSA) and chlorides: process optimization and kinetic modeling. Molecules. 2021;26(8):2208. doi: 10.3390/molecules26082208.
[41] Rakngam I, Osakoo N, Wittayakun J, Chanlek N, Pengsawang A, Sosa N, et al. Properties of mesoporous Al-SBA-15 from one-pot hydrothermal synthesis with different aluminium precursors and catalytic performances in xylose conversion to furfural. Micropor Mesopor Mat. 2021;317:110999. doi: 10.1016/j.micromeso.2021.110999.